






The manus of *Tetracynodon* (Therapsida: Therocephalia) provides evidence for survival strategies following the Permo-Triassic extinction

Gabriela Fontanarrosa, Fernando Abdala, Susanna Kümmell & Robert Gess

To cite this article: Gabriela Fontanarrosa, Fernando Abdala, Susanna Kümmell & Robert Gess (2018) The manus of *Tetracynodon* (Therapsida: Therocephalia) provides evidence for survival strategies following the Permo-Triassic extinction, *Journal of Vertebrate Paleontology*, 38:4, (1)-(13)

To link to this article: <https://doi.org/10.1080/02724634.2018.1491404>

 View supplementary material 

 Published online: 26 Mar 2019.

 Submit your article to this journal 

 View Crossmark data 



THE MANUS OF *TETRACYNODON* (THERAPSIDA: THEROCEPHALIA) PROVIDES EVIDENCE FOR SURVIVAL STRATEGIES FOLLOWING THE PERMO-TRIASSIC EXTINCTION

GABRIELA FONTANARROSA,*¹ FERNANDO ABDALA,^{2,3} SUSANNA KÜMMELL,⁴ and ROBERT GESS⁵

¹Instituto de Biodiversidad Neotropical, CONICET, Universidad Nacional de Tucumán, Crisóstomo Alvarez 722, San Miguel de Tucumán, Tucumán, Argentina, gab.fontanarrosa@gmail.com;

²Unidad Ejecutora Lillo, CONICET, Fundación Miguel Lillo, Miguel Lillo 251, San Miguel de Tucumán, Tucumán, Argentina;

³Evolutionary Studies Institute, University of the Witwatersrand, 1 Jan Smuts Avenue, Braamfontein 2000, Johannesburg, South Africa, nestor.abdala@wits.ac.za;

⁴Institute of Evolutionary Biology and Morphology, Center for Biomedical Education and Research, Faculty of Health, School of Medicine, University Witten/Herdecke, Alfred-Herrhausen-Strasse 50, 58448 Witten, Germany, susanna.kuemmel@uni-wh.de;

⁵Albany Museum and Geology Department, Rhodes University, 40 Somerset Street, Grahamstown 6139, South Africa, robg@imaginet.co.za

ABSTRACT—We present a comprehensive qualitative and quantitative study of the manus of a new therocephalian specimen referable to *Tetracynodon* from the Early Triassic of South Africa. We examined 18 specimens, representing at least 12 genera, including basal therocephalians (Lycosuchidae and Scylacosauridae) and eutherocephalians (Akidnognathidae, Whaitsioidea and Baurioidea). A temporal range of 23 million years through the Permo-Triassic (Wordian to Anisian) was surveyed. A principal component analysis of the therocephalian manus indicates that (1) metacarpals II, III, and IV acted as a module of which the medial and lateral elements (metacarpals I and V) were independent from each other; and (2) the proximal carpals, ulnare, and radiale lengths show contrasting variation in their measurements (e.g., groups with longer ulnares tend to have shorter radiales). The manus of Permian and Triassic taxa occupy separate regions in morphospace. This segregation pattern suggests selection for a manus with slender, elongated second to fourth metacarpals during and after the Permo-Triassic mass extinction. We show a heterogeneous condition of the fifth distal carpal bone. Although usually interpreted as fused to the fourth distal carpal or absent, the fifth distal carpal was present as a cartilaginous element in *Tetracynodon*. Strong and proportionally long unguals in relation to length of digits III and IV, wide and stocky basal phalanges, and short non-ungual phalanges strongly suggest that *Tetracynodon* was a scratch-digger. This supports the proposition that burrowing was an important behavioral strategy of terrestrial taxa during and after the Permo-Triassic mass extinction.

SUPPLEMENTAL DATA—Supplemental materials are available for this article for free at www.tandfonline.com/UJVP

Citation for this article: Fontanarrosa, G., F. Abdala, S. Kümmell, and R. Gess. 2019. The manus of *Tetracynodon* (Therapsida: Therocephalia) provides evidence for survival strategies following the Permo-Triassic extinction. *Journal of Vertebrate Paleontology*. DOI: 10.1080/02724634.2018.1491404.

INTRODUCTION

Therocephalia is an extinct clade of therapsids first represented in the middle Permian as large predators, the lycosuchids and the scylacosaurids (Abdala et al., 2008, 2014b). These taxa were replaced by a heterogeneous representation of small- to medium-sized insectivores and carnivores (Huttenlocker, 2014; Huttenlocker and Sidor, 2016) in the late Permian and even herbivores in the Triassic (Kemp, 1983; Abdala et al., 2014a). Therocephalians (in conjunction with dicynodonts and non-mammaliaform cynodonts) managed to survive the harsh environmental conditions during the Permo-Triassic extinction phase, only to become extinct during the Middle Triassic (Abdala et al., 2014a; Huttenlocker, 2014; Liu and Abdala, 2015).

The Permo-Triassic mass extinction is considered the most severe event of global biodiversity loss in Earth's history (Jablonsky, 2005; Roopnarine and Angielczyk, 2015). Environmental conditions in the terrestrial postextinction ecosystems are interpreted to have been characterized by high temperatures, aridity (Sun et al., 2012), low oxygen and high carbon dioxide pressure (Berner et al., 2007), and an unpredictable rainfall regime (Roopnarine and Angielczyk, 2015). In this context, burrowing is considered advantageous to survival for two main reasons: (1) fossorial animals are tolerant of hypoxic conditions, which are naturally present in burrows and Permian fossorial animals would therefore have been physiologically preadapted to low oxygen levels (Huttenlocker and Farmer, 2017); and (2) burrows provide a stable cool (thermal inertia) and more humid environment (Kinlaw, 1999). Thus, life in subterranean chambers provided crucial protection against the high temperatures and arid conditions prevalent in the Triassic (Botha-Brink, 2017; Huttenlocker and Farmer, 2017).

Therapsids have been found in small and large burrows in lower Triassic terrestrial rocks of the Karoo Basin in South

*Corresponding author.

Color versions of one or more of the figures in the article can be found online at www.tandfonline.com/ujvp.

Africa (Groenewald et al., 2001; Modesto and Botha-Brink, 2010; Bordy et al., 2011; Botha-Brink, 2017). Additionally, some of them show features associated with fossoriality, such as characteristic histological patterns of their bone microstructure (Botha-Brink et al., 2012; Huttenlocker and Botha-Brink, 2014; Huttenlocker and Farmer, 2017), cranial features (Cluver, 1978), and limb anatomy (Cox, 1972; Cluver, 1978; Botha-Brink, 2017).

The manus, being a structure intimately related to the interaction between an organism and its environment, shows extensive skeletal variation during the evolution of Tetrapoda (Flower, 1885; Hopson, 1995; Gates and Middleton, 2007; Polly, 2007; Kardong, 2011). The adaptive evolution of the manus allowed locomotion in a wide variety of physical environments, from land to water to air (Carroll and Holmes, 2007; Polly, 2007; Shapiro et al., 2007). As a result, features of the manus provide clues as to the ecological behavior of extinct taxa and are also useful in taxonomy. Nevertheless, just like other postcranial elements, the manus has received far less attention in therapsid evolutionary studies than the skull, possibly due to a bias in collecting (Rubidge, 2013).

A small-sized therocephalian specimen was recently found on the farm Carlton Heights, in the Pixley ka Seme District, Northern Cape Province, South Africa. It was recovered from strata of the Katberg Formation, corresponding to the lower Triassic *Lystrosaurus* Assemblage Zone. Preparation of the specimen revealed the skull and partial skeleton of a specimen of *Tetracynodon*, which shows pristine preservation, including a complete articulated manus. This small therocephalian genus, originally known from two specimens (one from the Upper Permian and the other from the Lower Triassic), was recently redescribed by Sigurdson et al. (2012). *Tetracynodon*, together with *Moschorhinus* and *Promoschorhynchus*, are the three therocephalian genera observed to have survived the Permian-Triassic mass extinction (Huttenlocker et al., 2011; Huttenlocker and Botha-Brink, 2013) and contributed to the survivor fauna.

Sigogneau's (1963) description of the holotype of *Tetracynodon darti* includes a partial manus, although several of its elements are moved out of their natural place. In their recently published morphological and paleobiological reassessment of *Tetracynodon*, Sigurdson et al. (2012) did not describe the holotypic manus in detail due to its earlier treatment by Sigogneau (1963).

In this contribution, we describe the manus of *Tetracynodon* specimen AM 3677 and present a comparison with that of the holotype of *Tetracynodon darti*. We provide a quantitative comparative survey of the skeletal morphology of the manus in therocephalians. Furthermore, we explore manus variation within a wide array of therocephalian taxa by utilizing principal component analysis of measurements of the component bones to generate a comparative morphospace. Finally, we assess the manual proportions for indicators of burrowing adaptation, which bestowed key ecological advantages for survival in a challenging postextinction environment.

Institutional Abbreviations—**AM**, Albany Museum, Grahamstown, South Africa; **BP**, Evolutionary Studies Institute (formerly Bernard Price Institute for Paleontological Research), University of the Witwatersrand, Johannesburg, South Africa; **CGS**, Council for Geosciences, Pretoria, South Africa; **NMQR**, National Museum, Bloemfontein, South Africa; **NHMUK**, Natural History Museum, London, U.K.; **RC**, Rubidge Collection, Wellwood, Graaff-Reinet District, South Africa; **SAM**, Iziko: South African Museum, Cape Town, South Africa; **TM**, Ditsong National Museum of Natural History (formerly Northern Flagship Institution: Transvaal Museum), Pretoria, South Africa; **UCMP**, University of California Museum of

Paleontology, Berkeley, California, U.S.A.; **UMZC**, University Museum of Zoology, Cambridge, U.K.

MATERIALS AND METHODS

Sample

Specimens examined first hand are listed by accession numbers, followed by references in which the particular specimen was described: *Glanosuchus macrops*: CGS RS 424, SAM-PK-K7809 (Fourie and Rubidge, 2009); Scylacosauridae indet.: BP/1/6228, BP/1/7655; *Ictidosuchooides longiceps*: BP/1/2294, BP/1/4092, CGS CM 86-655; *Scaloposaurus constrictus*: NMQR 3323; *Microgomphodon oligocynus*: SAM-PK-K10160 (Abdala et al., 2014a); *Mirotenthes digitipes*: UCMP 40467 (Attridge, 1956); *Olivierosuchus parringtoni*: BP/1/3849, BP/1/3973 (Fourie and Rubidge, 2007; Botha-Brink and Modesto, 2011; see the latter study for taxonomic reassessment of BP/1/3973); *Tetracynodon darti*: BP/1/2710 (Sigogneau, 1963); *Tetracynodon darti* AM 3677 (this work), UCMP 78395 (Sigurdson et al., 2012); *Theriognathus microps*: NMQR 3375, NHMUK R5694 (Boonstra, 1934); *Zorillodontops gracilis*: SAM-PK-K1392 (Cluver, 1969); *Eriolacerta parva*: UMZC T 369 (Watson, 1931); cf. *Eriolacerta*: BP/1/5895 (Damiani et al., 2003b); Baurioidea indet.: BP/1/4021; Therocephalia indet.: UCMP 40467; Therocephalia indet. juvenile: BP/1/6163.

Taxonomic Identification

The new specimen, AM 3677, comprises the complete skull with lower jaw in occlusion and the anterior portion of the skeleton. The preservation of the specimen is pristine (Fig. 2A), and several features permit assignment to *Tetracynodon*. Evident characteristics of the Lycideopidae include a long and narrow snout, an apparent nasal-lacrimal suture present on the left side, sutural connection between the maxilla and vomer forming a secondary palate, lack of a parietal foramen, and a long, gently curved lower jaw with a low coronoid process and presence of several incisors (Sigurdson et al., 2012). Other features present in AM 3677, such as the relatively smooth ventral surface of the pterygoid and absence of paired parasagittal ridges, suggest that AM 3677 is *Tetracynodon darti* (following Sigurdson et al., 2012).

Qualitative Data

A detailed analysis of the manus of *Tetracynodon* AM 3677 was carried out. We have taken into account the preserved components, their shapes and relative sizes, and their spatial arrangement. Specimen AM 3677 was furthermore compared with the manus of the holotype of *Tetracynodon darti* (BP/1/2710). Additionally, we surveyed the frequency of occurrence of the fifth distal carpal within a selected sample of therocephalian taxa.

Morphometric Data

A morphometric matrix was assembled based on the skeleton of the manus. We considered the proximodistal length and the lateromedial length (width) in most of the bones of the manus. In the case of metacarpals and phalanges, with variable widths along their extent, this measurement was taken over the central portion of the bone. Measurements of the preserved hand (either right or left) and the available surface (either ventral or dorsal) of the surveyed specimens (see Tables S1–S16, Supplemental Data) were taken with digital calipers.

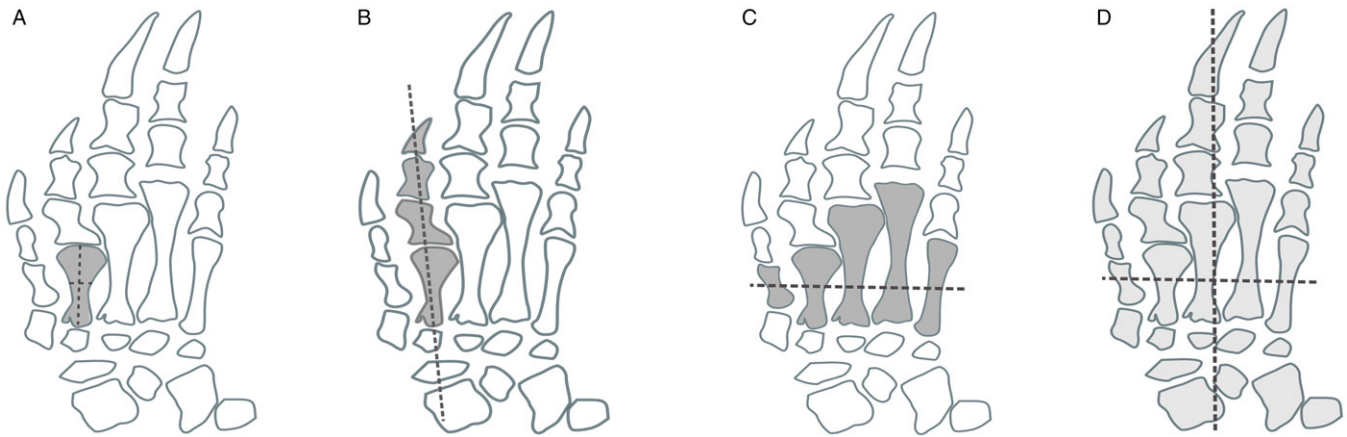


FIGURE 1. General schemes of the different analyses carried out in this study. **A**, comparison of intrinsic proportions of a single bone. The second metacarpal is shown in gray as an example. The dashed lines indicate the dimensions considered. **B**, comparison of segment lengths within a ray. The elements of the second ray are shown in gray as an example. The dashed lines indicate the dimension considered. **C**, comparisons of the regions: the regions are delimited according to their location in the proximodistal axis and are composed of serial adjacent segments. The elements pertaining to the metacarpal region are shown in gray as an example. The dashed line crosses all the elements of the same region. **D**, the manus as a whole, considering both axes (dashed lines) of arrangement. All the bone elements of the hand are shown in gray. The dashed lines indicate the dimensions considered.

We also analyzed a second data set, assembled by Weisbecker and Warton (2006) and Kümmell (2009), regarding length and width of the basal phalanx of the fourth digit in both extant mammals and extinct therapsids (dicynodonts, non-mammaliaform cynodonts, therocephalians). The data set includes functional assignation of living taxa (arboreal, digger, scansorial, terrestrial, terrestrial-digger) and putative inferred function for fossil taxa (probably terrestrial, probably terrestrial-digger).

Qualitative Data Analysis

We have created schematics of the patterns of the carpometacarpal line and metacarpophalangeal line. These take the form of the virtual lines connecting the series of carpometacarpal joints and metacarpophalangeal joints of each ray of the hand.

Morphometric Data Analysis

We organized the data analysis according to four different criteria (Fig. 1):

1. Intertaxonomic comparisons of intrinsic properties of a single bone: length-to-width index of distal carpal 1. This bone was selected for its relatively high variability within the therocephalian sample. Following Kümmell (2009) and Kümmell and Frey (2012), we also included a comparison of the index of width to length of the basal phalanx of digit IV, as a proxy for locomotive mode. For the latter, we also included non-mammaliaform cynodonts, extant monotremes, diprotodontid marsupials (Weisbecker and Warton, 2006), and placentals. This analysis combined new information on therocephalians with data previously analyzed by Kümmell (2009:fig. 85) and Kümmell and Frey (2012:fig. 1).
2. Intrinsic comparisons of segment lengths within a ray: the rays in the manus are composed of proximal to distal serial segments. We compared the lengths of metacarpal III (McIII) and basal phalanx III (BP3) with their total combined length. Lengths of both bones were added, and then

the proportion of each bone to the total length was calculated. These bones were selected due to their relatively high frequency of preservation in the sample.

3. Intrinsic comparisons of the manus regions: we considered the regions of the manus delimited according to their location in the axis. Thus, the regions are composed of adjacent segments: e.g., McI, McII, McIII, McIV, and McV. We compared the relative lengths of each metacarpal of the manus and compared the McIII length/McII length and McIV length/McI length indices.
4. The manual skeleton as a whole: considering both axes of arrangement.

In order to reduce the dimensionality of the data set and to simplify the organization of variables, we used the whole manus matrix to perform a principal component analysis (PCA). The PCA constructs a linear transformation into a new coordinate system in which the highest variance of the data set is captured by the first axis (PC1), the second highest variance is captured by the second axis (PC2), and so on. This helps us to establish sources of variation in the data set and to order them by their relative importance. As a result, we obtained a biplot chart (morphospace) that simultaneously shows the spatial distribution of the specimens under study in the new coordinate system and also how the original variables correlate with the synthetic variables (principal components). The PCA is not able to deal with missing data, requiring a complete matrix. Although this requirement is difficult to attain with fossil samples, it is possible to replace missing data by the arithmetic mean of the variable for the whole sample. Thus, it is possible to perform a PCA without deleting variables or specimens. The effective bias, if any, results in shifting specimens nearer to the center of the morphospace. The morphospace was constructed based on a selected group of variables from the original data in order to minimize missing data in the matrix (see Table 1). In addition, the geological period of provenance of each specimen was considered. All statistical analyses were implemented in the R statistical environment (R Development Core Team, 2011).

RESULTS

Description of the Manus of AM 3677

The right manus of AM 3677 is nearly complete and exposed in dorsal view (Fig. 2). Preserved elements are radiale, ulnare, pisiform, medial and lateral centrale, and distal carpals 1, 2, 3, and 4. Metacarpals and digits are complete and fully articulated. The phalangeal formula is 2-3-3-3-3.

The ulnare is rectangular in dorsal view, with a small thinning in the central portion. It is anteroposteriorly elongated, medially displaying a proximodistally oriented concavity, which is pronounced in its central portion. The lateral centrale, located distomedially to the ulnare, is rectangular, half the width of the ulnare, and approximately one-third of the width of the radiale.

TABLE 1. Correlation of each variable considered for the first (PC1) and second (PC2) principal components (i.e., their loadings).

Variable	PC1 (34%)	PC2 (16%)
Metacarpal IV length	-0.483	0.028
Metacarpal III length	-0.478	0.018
Radiale length	-0.309	0.599
Distal carpal 4 width	0.289	0.034
Metacarpal V length	-0.282	-0.004
Metacarpal II length	-0.243	-0.162
Digit III, phalanx I length	0.180	0.145
Distal carpal 4 length	0.171	0.086
Digit IV, phalanx I length	-0.138	0.259
Metacarpal II width	0.134	0.024
Ulnare length	-0.127	-0.436
Metacarpal I width	0.121	-0.010
Digit V, phalanx I length	-0.113	-0.126
Ulnare width	-0.107	0.023
Digit I, phalanx I length	0.106	0.101
Digit III, phalanx I width	0.106	0.040
Metacarpal I length	0.100	0.050
Radiale width	-0.093	-0.179
Digit V, phalanx I width	-0.092	-0.187
Digit II, phalanx I width	0.082	-0.005
Digit IV, phalanx I width	0.074	0.295
Metacarpal III width	0.049	-0.060
Digit I, phalanx I width	0.034	0.31
Digit II, phalanx I length	-0.027	-0.022
Metacarpal IV width	0.026	-0.013
Metacarpal V width	0.004	-0.200

The variables are in descending order of their absolute correlation values in PC1.

The dorsally convex radiale is one-third shorter than the ulnare. Its medial margin is slightly shorter than its lateral one. There is no contact between ulnare and radiale. The pisiform is circular in dorsal view and contacts the proximolateral margin of the ulnare. It is nearly half the size of the ulnare. The medial centrale is rectangular, with its major axis perpendicular to the manual axis. It has the same width as the radiale and is the proximodistally shortest element of the proximal and central carpals. Distal carpal 1 is the largest of the distal elements. It is rectangular, with the major axis parallel to the manual axis, and has a particularly flat dorsal surface. Distal carpal 2 is slightly displaced, with its dorsal surface approximately quadrangular. Distal carpals 2 and 3 are the smallest preserved elements of the carpus. Distal carpal 4 is quadrangular and flat and is the second largest distal carpal. The metacarpals display a progressive lengthening of the elements from I to IV (Fig. 3A). The McV is shorter, with a length intermediate between those of McII and McIII. The distal margins of these bones are wider than the proximal margins. The arch formed by the articulations between the distal carpals and metacarpals (carpometacarpal line) gradually increases distally from ray II to ray IV, whereas the articulation between distal carpal 1 and McI is displaced distally (Fig. 3A). Basal phalanges are subequal in length, rectangular in dorsal view, short and robust, with their long axis aligned to the ray axis. The surface of the phalanges is convex in cross-section and smooth. The proximal margins of these bones are slightly wider than the distal margins. The arch of the articulation between metacarpals and basal phalanges (metacarpophalangeal line) increases steadily from ray I to ray IV and decreases from ray IV to ray V. The articulation between the metacarpals and basal phalanges is represented by a convex joint facet of the metacarpal heads and a concave articulation surface at the proximal end of the basal phalanges, forming a roller joint. The intermediate phalanges are hourglass-shaped. The proximal interphalangeal joint seems to be of a compressed ellipsoid type. These phalanges are subequal in length, except the intermediate phalanx of digit V, which is shorter. Digit I presents the shortest ungual phalanx. The ungual phalanges increase in length in the following order: I < II < V < IV < III; III is extraordinarily long. The ungual phalanges articulate with the intermediate phalanges with hinge-type joints, the proximal portion of the ungual phalanx being superposed on the dorso-distal margin of the intermediate phalanges. The ungual phalanges are laterally compressed and show a slight dorsal curvature (Fig. 2B).

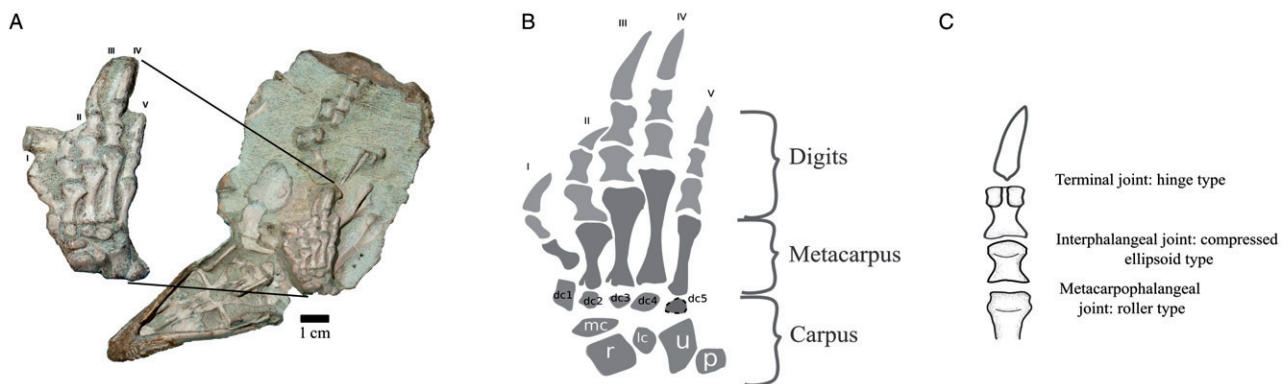


FIGURE 2. *Tetracynodon* AM 3677. **A**, photograph of ventral view of specimen with right manus seen in dorsal view, with manus enlarged on the left. The manual rays are shown in roman numbers. **B**, scheme of the right manus in dorsal view with nomenclature of the manual bones. **C**, scheme of the digital joint types. **Abbreviations:** **dc1**, distal carpal 1; **dc2**, distal carpal 2; **dc3**, distal carpal 3; **dc4**, distal carpal 4; **dc5**, distal carpal 5 (absent, interpreted as cartilaginous and indicated with dash lines); **lc**, lateral centrale; **mc**, medial centrale; **p**, pisiform; **r**, radiale; **u**, ulnare.

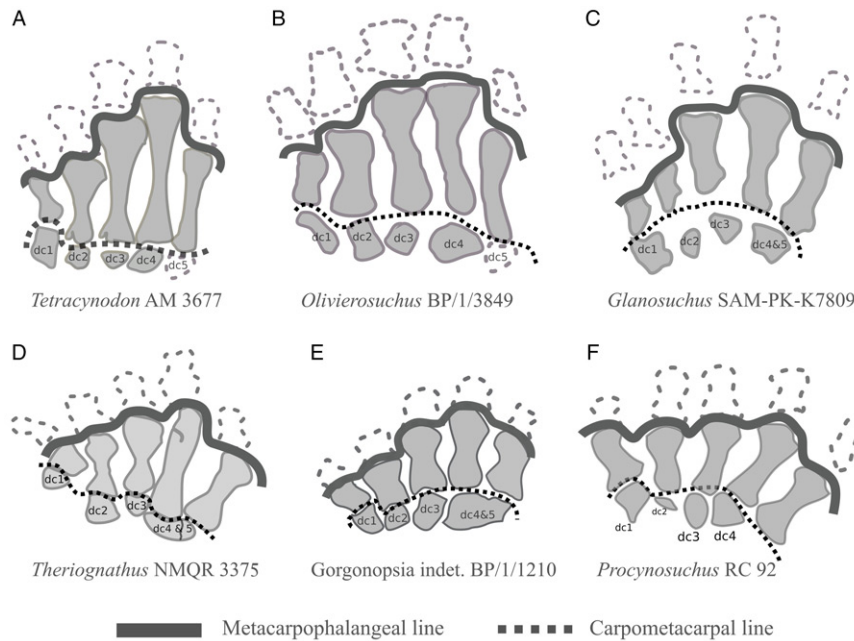


FIGURE 3. Schemes of the carpometacarpal and metacarpophalangeal lines of different therocephalids. **A**, *Tetracynodon darti* AM 3677. **B**, *Oliverosuchus parringtoni* BP/1/3849. **C**, *Glanosuchus macrops* SAM-PK-K7809. **D**, *Theriognathus microps* NMQR 3375. **E**, *Gorgonopsia* indet. BP/1/1210. **F**, *Procynosuchus delaharpeae* RC 92. Not to scale. **Abbreviations:** **dc1**, distal carpal 1; **dc2**, distal carpal 2; **dc3**, distal carpal 3; **dc4**, distal carpal 4; **dc4&5**, fused distal carpals 4 and 5; **dc5**, distal carpal 5.

Comparison of AM 3677 with the Manus of *Tetracynodon darti* Holotype

The holotype of *Tetracynodon darti* (BP/1/2710) preserves a partial manus that was described by Sigogneau (1963). We interpret the bone identified as a radiale by Sigogneau (1963) as the ulnare and vice versa. She labeled a large bone located in front as the radiale and the ulnare as the intermedium (Sigogneau, 1963:fig.4a), but in the description she mentions that the intermedium is located distal to the radiale and the ulnare, coinciding with the bone that we interpret as intermedium.

In BP/1/2710, distal carpal 1 is rectangular and clearly more elongated proximodistally than in AM 3677 (Fig. 4). In both specimens, McI is situated more distally than the remaining metacarpals (see Fig. 3A). As in *Tetracynodon* AM 3677, distal carpal 5 is absent in the holotype of *T. darti*, but in both specimens there is a long space between the ulnare and the McV. Distal carpal 1 is larger than distal carpal 4. The index between the McIV and McV lengths is similar in both specimens. The ungual phalanx of digit I is longer than the intermediate phalanges of the remaining digits in both specimens. There is also a similar extreme widening of the distal margin of McII and McIII in both *Tetracynodon* specimens.

The comparison of the ulnare highlights some noteworthy differences between the two specimens. However, our identification of this bone in BP/1/2710 is tentative, because we interpret the bone in this specimen as rotated 180°, so that it is out of place regarding its orientation. The manus of BP/1/2710 is prepared dorsally, but we consider the ulnare to be exposed in ventral view instead. A major difference is that the ulnare of BP/1/2710 appears to be comparatively longer than the same element of AM 3677, which shows a more complex surface.

Arrangement Patterns: Carpometacarpal Line and Metacarpophalangeal Line

In almost every specimen shown in Figure 3, the most distal joint of the carpometacarpal line belongs to the joint in the

first ray, although in *Glanosuchus* the most distal joint is the third one (Fig. 3C). The most distal joint in the metacarpophalangeal line is that of the fourth ray, and the most proximal is the joint of the first ray.

In *Tetracynodon* (Fig. 3A), the arch formed by the carpometacarpal joints show a pronounced distal displacement of the first distal carpal. The carpometacarpal joints of the second to fourth ray are aligned in a straight line perpendicular to the longitudinal axis of the manus. In *Oliverosuchus* (Fig. 3B), the pattern is similar to *Tetracynodon*, but McV is located more proximally. In *Glanosuchus* (Fig. 3C), the arch rises gradually from the first to the third joint and then decreases until the fifth ray. The distal displacement of the first distal carpal is remarkable in *Theriognathus*, whereas the most proximal placement of the carpometacarpal line is in the fourth ray (Fig. 3D). However, these extreme positions might be due to the fact that both McI and McIV are somewhat displaced in this fossil. The pattern of the carpometacarpal line outside Therocephalia is here exemplified by the gorgonopsian BP/1/1210 (Fig. 3E) and the basal non-mammaliaform cynodont *Procynosuchus* (Fig. 3F), in which the displacement of the first carpometacarpal joint is also present.

In *Tetracynodon* and *Theriognathus*, the metacarpophalangeal line increases gradually from the first to the fourth ray and then decreases to the fifth ray (Fig. 3A, D). In *Oliverosuchus*, the arch rises gradually from the first to the third ray, with no further growth to the fourth ray, and then decreases to the fifth ray (Fig. 3B). In *Glanosuchus*, there is almost no change between the lengths of the first and second metacarpals, but a remarkable difference between the second and third metacarpals (Fig. 3C). The metacarpal length continues increasing until the fourth element and then decreases to the fifth one. In *Theriognathus*, the metacarpophalangeal line rises gradually from the first to the fourth joint and then decreases until the fifth ray (Fig. 3D).

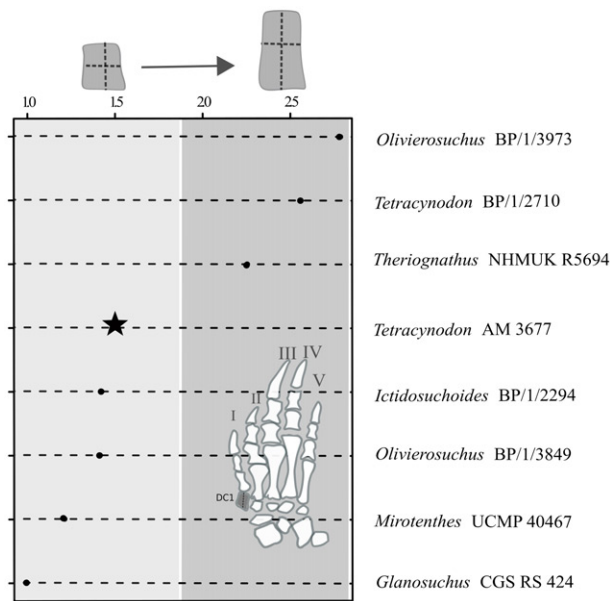


FIGURE 4. The intrinsic index of the first distal carpal (distal carpal 1 length/width) of Therocephalia. The star represents the value of the focal *Tetracynodon* specimen.

The gorgonopsian BP/1/1210 presents a small difference between the position of the distal end of McI and McII, then the third and fourth metacarpals have the same length, followed by a small decrease of the metacarpophalangeal line towards the fifth metacarpal (Fig. 3E). The basal non-mammaliaform cynodont *Procynosuchus* shows a less stepped metacarpophalangeal line in which the first to fourth metacarpals are similar in length and the fifth element is slightly shorter (Fig. 3F).

Morphometric Data

Morphology of the Distal Carpal 1—There is a trend towards bimodality in the length-to-width index of the distal carpal 1 (length/width = carpal I index), but the values are highly variable for specimens of the same taxon, such as those of the taxa *Tetracynodon* and *Olivierosuchus* (Fig. 4). The carpal I index of *Glanosuchus* is close to 1 (i.e., it is isodiametric), whereas the other extreme is represented by *Olivierosuchus* BP/1/3973 and *Tetracynodon* BP/1/2710, which have an elongated distal carpal 1, showing a high index (close to 1.5). *Tetracynodon* shows great variation, with the distal carpal 1 appearing proportionally longer in BP/1/2710 than in AM 3677.

Basal Phalanx 4—The length/width index (LWI) of the basal phalanx of the fourth digit shows negative allometry (slope of 0.75 for Therocephalia), so larger animals usually have lower LWI values than smaller animals with the same locomotor mode (Kümmell, 2009) (Fig. 5A). The LWI of *Tetracynodon darti* AM 3677 is 1.79. It belongs to the lower range of LWI values for small Therocephalia, because other small Therocephalia show values between 1.99 and 2.31. The LWI values of the digging non-mammaliaform cynodont *Thrinaxodon* are much higher (2.81–4.38) than in *Tetracynodon*. Among extant animals, the LWI of *Tetracynodon* (LWI = 1.79) is between that of the diprotodontid marsupials *Bettongia penicillata* (LWI = 1.61) and *Potorous* (LWI = 1.5) on the one hand and *Lagorchestes hirsutus* (LWI = 2.31) and *Onychogalea lunata* (LWI = 2.67) on the other, but closer to the former two. All four specimens have a basal

phalanx IV length similar to that of *Tetracynodon* AM 3677, indicating that they are all of a similar size range. *Bettongia penicillata* and *Potorous* are terrestrial and dig for food, whereas *Lagorchestes* and *Onychogalea lunata* were categorized by Weisbecker and Warton (2006) as fully terrestrial (Fig. 5B).

Index between the Lengths of Metacarpal III and Basal Phalanx III—In all studied specimens of Therocephalia, McIII length accounts for at least 50% of the combined length of McIII and basal phalanx III, and in the majority of cases the length of this element contributes more than 60% of the combined length. In the majority of examples, the first phalanx length accounts for more than 30% of the combined length of the two bones (Fig. 6). The relatively shortest metacarpals (little more than 50% of the combined length) are found in *Mirotenthes* and in the Scylacosauridae indet. BP/1/6228. In the case of *Mirotenthes*, it should be noted that McIII is very deformed and has been dorsoventrally crushed. The relatively longest metacarpals are found in three Triassic taxa: *Olivierosuchus* BP/1/3849 and two baurioids: *Tetracynodon* AM 3677 and *Microgomphodon* SAM-PK-K10160. In these examples, the metacarpal accounts for 70% or more of the combined length of the elements.

Intrinsic Comparisons of the Manual Regions

Relative Metacarpal Lengths—When the complete metacarpus is preserved, the longest element in Therocephalia is always McIV and the shortest McI, with the second shortest being McII. The third longest bone is McV in *Tetracynodon* AM 3677 (Fig. 7B), *Glanosuchus* SAM-PK-K7809 (Fig. 7A), and the basal baurioid BP/1/4021 (Fig. 7C). On the other hand, the third longest metacarpal of *Theriognathus* is McIII (Fig. 7E). In *Ictidosuchooides* and *Olivierosuchus*, McIII and McV are subequal (Fig. 7C, D). We found extreme differences in the two specimens of *Theriognathus*, with the largest specimen, NHMUK R5694, showing greater contrast between the lengths of McII to McIV (Fig. 7E). The other *Theriognathus* specimen, NMQR 3375, is the only case noted in our survey with relative equalization of the metacarpals, with small differences in length from McII to McV (Fig. 3D).

Metacarpal IV/Metacarpal I Index—The ordered values of the McIV/McI index can be separated into three ranges (Fig. 8). The genera in the lowest range, with values of the index ranging from 1.8 to 2.2 (the smallest differences between the lengths of these metacarpals), are *Theriognathus* NHMUK R5694 and *Microgomphodon* SAM-PK-K10160. Genera in the intermediate range, with values between 2.4 and 2.6, are *Glanosuchus* CGS RS 424, *Mirotenthes* UCMP 40467, and *Tetracynodon* AM 3377. Genera in the highest range, with values between 2.8 and 3.2 (the largest differences between the lengths of McIV and McI), are *Theriognathus* NMQR 3375, cf. *Erciolacerta* BP/1/5895, the indeterminate therocephalian BP/1/6163, and *Tetracynodon* BP/1/2710. There are, therefore, some cases with marked variations in the values of specimens representing the same genus, notably *Tetracynodon* and, more drastically, *Theriognathus*.

Metacarpal III/Metacarpal II Index—The McIII/McII index value derived from a single specimen is shown with a vertical line in Figure 9. Whenever two or more specimens per genus were available, values are represented by a box plot. The taxa are ordered along the x-axis according to decreasing index values. The star represents the value for *Tetracynodon* AM 3677.

The ordered values can be separated into three ranges. Taxa with values from 1.2 to 1.3 are *Theriognathus*, *Ictidosuchooides*, *Microgomphodon*, *Tetracynodon darti* (AM 3677), and *Mirotenthes*. Genera in the second range, with values around

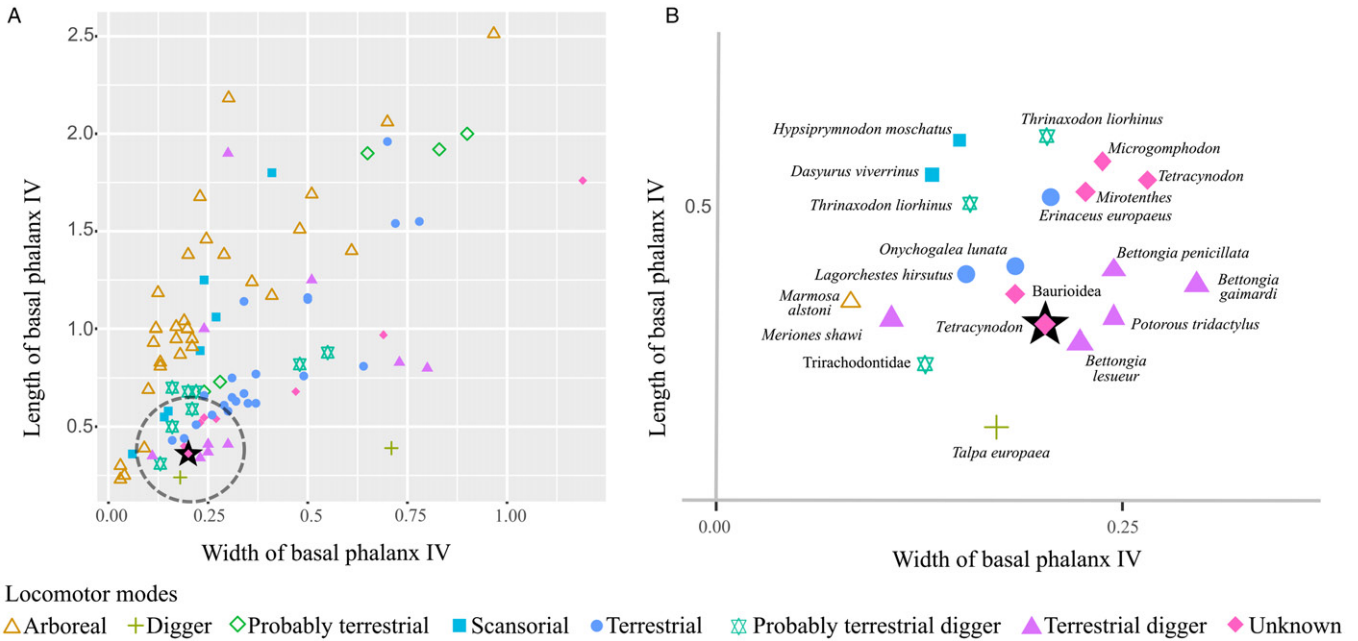


FIGURE 5. Index of the basal phalanx of the fourth digit. **A**, scatter plot in which each point represents the basal phalanx length (vertical axis) and width (horizontal axis) values of the basal phalanx of the fourth digit of members of therocephalians, non-mammaliaform cynodonts, and mammals. The symbols indicate different locomotor modes. The star represents the focal specimen *Tetracynodon darti* AM 3677. The dash lined circle represents the area of the scatter plot that is magnified in **B**. **B**, close-up of **A** centered on the focal specimen *Tetracynodon darti* AM 3677.

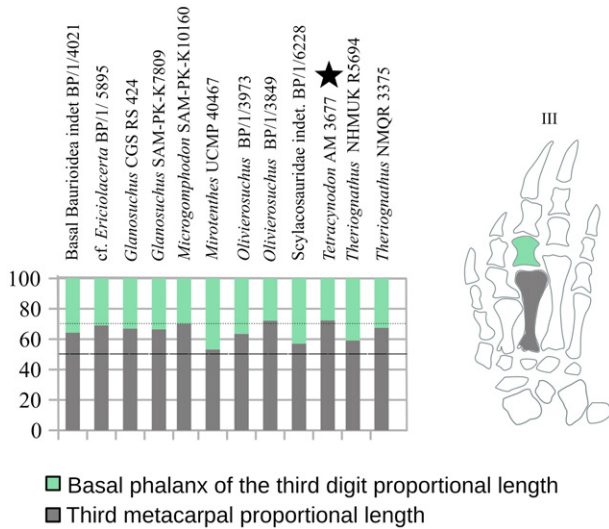


FIGURE 6. Relative lengths of the metacarpal and the first phalanx of the third ray. The graph shows the length of each bone as a percentage of the combined total length. The dotted line indicates the upper limit of metapodial length (70%) and the dashed line the lower limit (50%). The star marks the focal specimen *Tetracynodon* AM 3677.

1.5, are *Olivierosuchus*, Scylacosauridae, basal Baurioidea indet., and *Tetracynodon darti* UCMP 78395. Genera in the third group, with values around 1.7, are *Glanosuchus* and cf. *Ericiolacerta*. *Glanosuchus* shows relative large variation between specimens (1.4 to 1.8).

The Manual Skeleton as a Whole: Therocephalian Manual Morphospace—The first two axes of the morphospace (PC1 and PC2) derived from the principal component analysis

account for only 50% of the morphometric variation (34% and 16%, respectively). Additionally, our analysis reports high correlations between our original variables and the synthetic ones. This is demonstrated graphically as long vectors in Figure 10B (see also Table 1).

Most of the specimens are distributed over PC1, with low absolute scores of PC2 (Fig. 10A). Exceptionally, *Microgomphodon* SAM-PK-K10160 is far from the PC1 axis, reaching the largest value on PC2 (row coordinates = -0.34; 0.30), whereas cf. *Ericiolacerta* BP/1/5895 is also far from PC1, having the lowest value of PC2 (row coordinates = -1.13; -0.39). The first principal component separates two main groups categorized by geological age: all Triassic specimens are located in an area with values of approximately 0 or less, whereas all Permian ones are located in an area with values of approximately 0 or greater (see minimal polygons drawn over the specimens in Fig. 10A). The main variables that contribute to the separation between these temporal groups are width of the radiale, McIV length, McIII length, McV length, distal carpal 4 length, and McII length. The manus of Permian therocephalians is characterized by short McII, McIII, McIV, and McV and by a narrow radiale, whereas in the Triassic forms those bones are respectively longer and wider (Fig. 10B).

The Triassic forms are widely distributed along a gradient over PC2. The one extreme, *Microgomphodon* SAM-PK-K10160 from the Middle Triassic, has a long ulnare and a wide McV. At the opposite extreme of the gradient, cf. *Ericiolacerta* BP/1/5895 shows a long basal phalanx IV and a wide radiale. Permian forms are mainly distributed in a gradient over PC1. At one extreme is *Theriognathus* NMQR 3375, characterized by intermediate values of the length of the ulnare and relatively wide McV. At the opposite extreme, the unidentified scylacosaurid BP/1/7655, has a long basal phalanx III and short metacarpals.

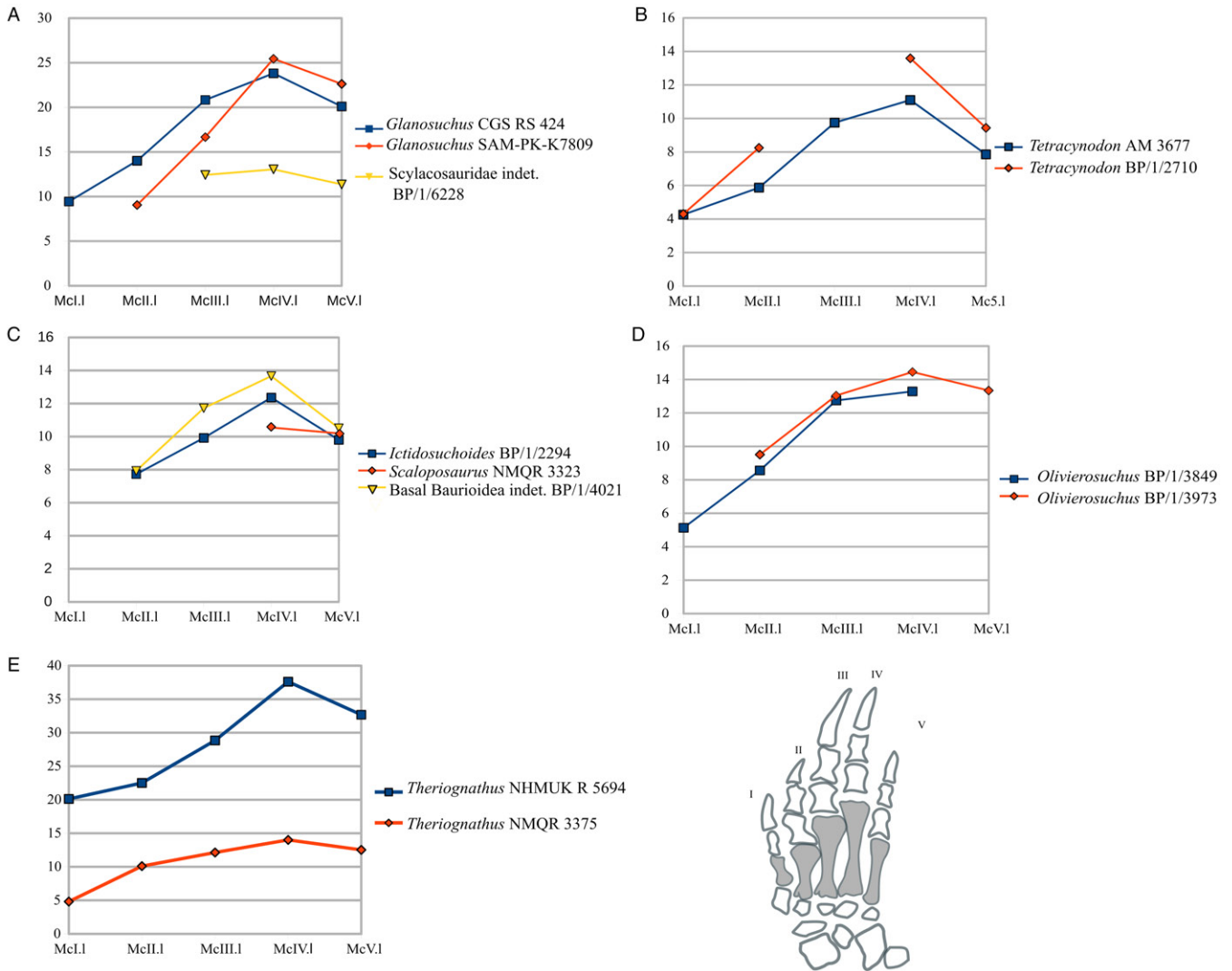


FIGURE 7. Absolute length in mm of each metacarpal in Therocephalia. **A**, *Glanosuchus macrops* and an unidentified Scylacosauridae. **B**, *Tetracynodon darti*. **C**, Baurioidea. **D**, *Olivierosuchus parringtoni*. **E**, *Theriognathus microps*. **Abbreviations**: **McI.I**, metacarpal I length; **McII.I**, metacarpal II length; **McIII.I**, metacarpal III length; **McIV.I**, metacarpal IV length; **McV.I**, metacarpal V length.

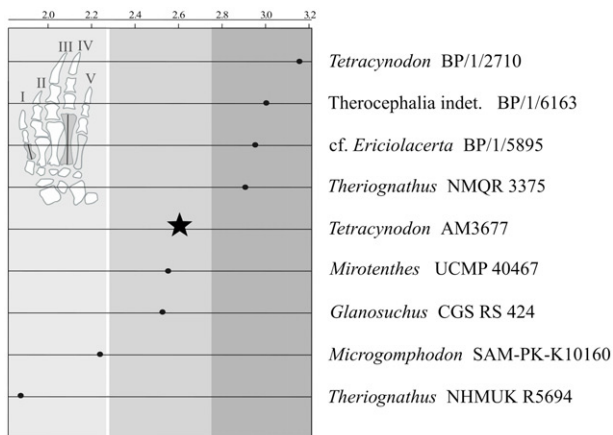


FIGURE 8. Index between the length of McIV and the length of McI. The star represents the value for *Tetracynodon* AM 3677. **Abbreviations**: **McI**, metacarpal I; **McIV**, metacarpal IV.

DISCUSSION

Therocephalian Morphological Variation

The therocephalian manus exhibits wide variability, which is most evident in the relative lengths of the metacarpals, ulnare, radiale, and distal carpal 4, and in the width of the radiale (Fig. 10B). The manus of *Tetracynodon* specimens occupies an extreme position on PC1 in the morphometric space. This placement results from the manus having relatively long metacarpals and a wide radiale. At the opposite extreme, the manus of the unidentified scylacosaurid, BP/1/7655, has relatively short metacarpals, a narrow radiale, and a long fourth distal carpal. *Microgomphodon* SAM-PK-K10160 has an extreme position on PC2 with a long ulnare, whereas at the other extreme cf. *Erciolacerta* BP/1/5895 has a relatively long radiale. The variation along PC2 for Permian therocephalians is less than that for Triassic taxa (Fig. 10A).

The morphospace shows that metacarpals II, III, and IV of Therocephalia in general behave as a module, having a coherent morphological trend, both in length and width, with a unified direction of growth. It is worth noting that the only

metacarpals showing a contrary trend are the most lateral and medial ones. In terms of metacarpal width, McV is the only one decoupled in the metacarpal series, and in terms of length,

McI is the only one decoupled in the series of McI to McIV (Fig. 10B).

Among the proximal carpals, the ulnare and the radiale behave as independent structures because they increase in opposite directions (both regarding length and width). Specifically, taxa with long ulnares have high positive values for PC2 and taxa with a long radiale have a high negative value instead (Fig. 10B).

The preservation of several specimens that include the manus of *Tetracynodon*, *Glanosuchus*, *Olivierosuchus*, and *Theriognathus* represents an excellent opportunity for exploring aspects of taxonomic and intrageneric variation in Therocephalia.

The manus of *Tetracynodon* is long and slender, with particularly long metacarpals and ungual phalanges. The main differences between the two specimens included in this taxon are the more elongated radiale (Fig. 10B) and first distal carpal in BP/1/2710 (Fig. 4). The specimens show a similar pattern of metacarpal lengths (Fig. 7B).

In *Theriognathus*, the manus is broad and short, although comparatively longer than that of *Glanosuchus*, with the ungual phalanx constituting the longest element. Small variations, on the order of less than 10%, are seen in the relative lengths of McIII and the first phalanx of digit III in *Theriognathus* (Fig. 6). The length of the metacarpals is extremely variable in *Theriognathus*, with the difference between the lengths of McIV and McV clearly more marked in the largest specimen NHMUK R5694 (Fig. 7E) than in NMQR 3375. Patterns of metacarpal lengths in *Tetracynodon* and *Olivierosuchus* show similarities in the sampled specimens (Fig. 7B, D).

In *Glanosuchus*, the manus is moderately broad and has conspicuously short digits. There is a proximodistal elongation of the ulnare that enables articulation of this bone with McV and accounts for the absence of distal carpal 5. The relative values between McIII and the first phalanx of digit III in *Glanosuchus* specimens CGS RS 424 and SAM PK K7809 are similar (Fig. 6). Comparison of the lengths of the metacarpals in these two

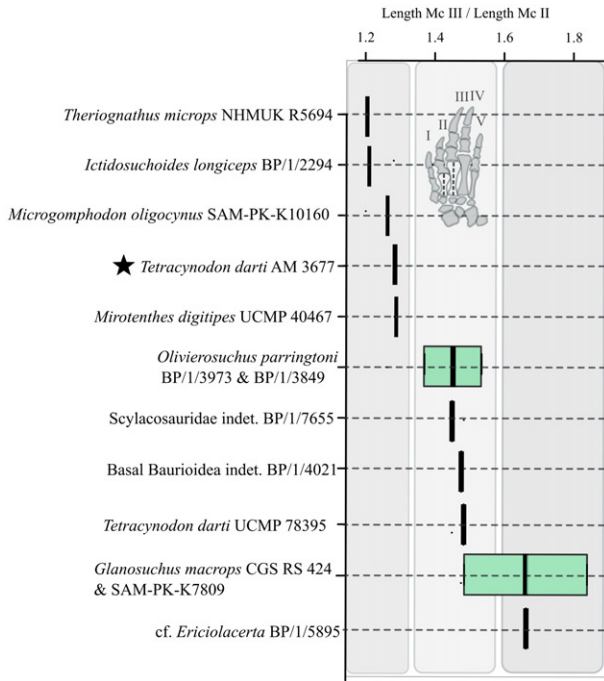


FIGURE 9. Index between the length of McIII and the length of McII. The genera are arranged by the values of the index in ascending order. In a few cases, shown in box plots, the information is derived from more than one specimen. The star represents the focal specimen *Tetracynodon* AM 3677.

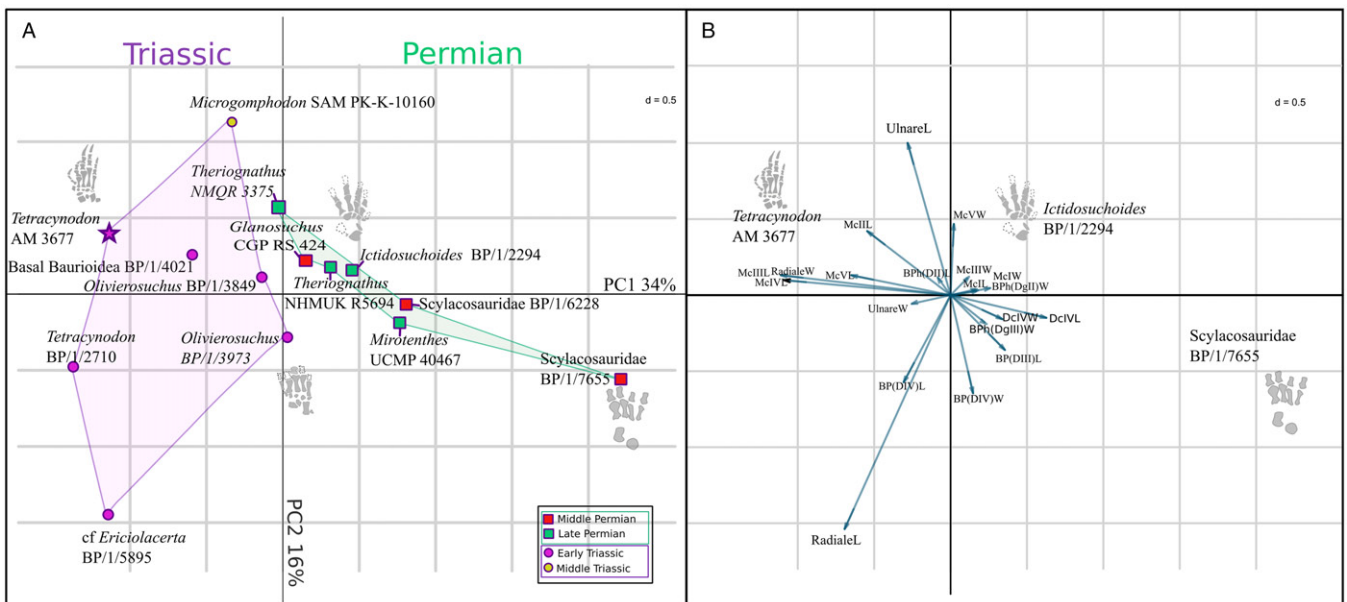


FIGURE 10. Therocephalian manual morphospace based on a principal component analysis (PCA). **A**, plot of the specimens distributed in the manual morphospace. Purple-shaded area indicates Triassic taxa. Green-shaded area indicates Permian taxa. The star represents *Tetracynodon* AM 3677. **B**, plot of the contribution of the original variables used to construct the synthetic variables. Graphical scale of the grid equals 0.5.

specimens shows a generally similar pattern, but McII and McIII are slightly longer in CGS RS 424, whereas McIV and McV are slightly longer in SAM-PK-K7809 (Fig. 7A).

In *Olivierosuchus*, the manus is also broad with short phalanges. A major apparent difference between the specimens of this taxon is the morphology of distal carpal 1, which is a massive quadrangular bone in BP/1/3849, whereas it appears to be a tiny anteroposteriorly elongate element in BP/1/3973. This difference may derive from the displacement of this element in BP/1/3973, such that the medial surface of the bone is exposed, rather than the dorsal surface. There is also a small variation, on the order of less than 10%, in the relative lengths of the McIII and first phalanx of digit III (Fig. 6).

Distal Carpal 5 Variation

Boonstra (1964) and Hopson (1995) reported, that in Therocephalia the fifth distal carpal was fused to the fourth distal carpal to form a single big element. In this study, we show that the situation is more complex. When the bone is absent, the fourth distal carpal is often a large, mediolaterally expanded element that articulates with the fourth and fifth metacarpals. In these cases, the most parsimonious interpretation is the fusion of the fourth and fifth distal carpals (see *Glanosuchus* and *Theriognathus* in Fig. 3C, D). In humans, the fourth distal carpal forms the hamate (Cihák, 1972) and is usually the largest distal carpal, and in several living mammals the fourth distal carpal articulates with McIV and McV (Holmgren, 1952; Weisbecker and Sánchez-Villagra, 2006; Prochel et al., 2014). A different condition of the fifth distal carpal is seen in *Tetracynodon* AM 3677 (see Fig. 2). In this specimen, the fourth distal carpal articulates only with McIV, and there is an empty space in the expected position of a fifth distal carpal, which is interpreted here as being a cartilaginous element in the living animal (Fig. 2B). Confirmation of this condition in the other *Tetracynodon* specimen (BP/1/2710) was precluded due to taphonomic disturbance of the bones. Nonetheless, this character is potentially taxonomically important. A corresponding empty space has also been noted in dicynodonts and some eucynodonts (Hopson, 1995) (see below).

Four distal carpals, interpreted as a result of the fusion of the fourth and fifth ones, as is seen in most therocephalians, are also recognized in biarmosuchians and gorgonopsians, and forms with either four or five elements are found in anomodonts and non-mammaliaform cynodonts (Hopson, 1995; Fröbisch and Reisz, 2009, 2011; Kümmell, 2009).

When discussing the empty space for distal carpal 5 in dicynodonts and some eucynodonts, Hopson (1995) interpreted this condition as a lack of ossification of this element. As comparison, he asserted that in lizards the fifth distal carpal is one of the last elements of the carpus to ossify during ontogeny and one of the first to be lost in phylogeny (Rieppel, 1992). This ossification pattern argument regarding the loss of the fifth distal carpal is, however, flawed due to misrepresentation of the developmental sequence in Squamata. Although the cartilage condensation that will form the fifth distal carpal in the early embryonic stages of Squamata is delayed relative to those associated with the other distal carpals, the later ossification process occurs in all distal carpals simultaneously (see Fabrezi et al., 2007:fig. 9b). There are no characteristics of *Tetracynodon* AM 3677 that might support a juvenile status for the specimen. Extant squamates therefore do not provide any analogous ontogenetic stages that might explain the osteological features observed in *Tetracynodon* AM 3677, some dicynodonts, and some eucynodonts (Shubin and Alberch, 1986; Fabrezi et al., 2007). It is, therefore, more plausible that *Tetracynodon* AM 3677 is, in fact, an adult specimen with a cartilaginous distal carpal 5.

Distal Carpal 1

Within Therocephalia, distal carpal 1 is an element that is particularly variable in terms of shape and size. This bone ranges from being one of the smallest distal carpals in *Theriognathus* (Fig. 3D) to the largest in *Tetracynodon* (Fig. 3A). In terms of its intrinsic proportions, distal carpal 1 is almost a bimodal element with two extreme morphological conditions: a quadrangular bone or a proximodistally elongated bone (i.e., rectangular). It is important to highlight the inconsistency of this character within the taxa in our sample: different specimens of *Tetracynodon* and *Olivierosuchus* appear to exhibit both types of distal carpal 1 (Fig. 4). We have no explanation for this difference between *Tetracynodon* specimens. In the case of *Olivierosuchus*, it is possible that the distal carpal 1 in BP/1/3973 is displaced and partially covered, such that the lateromedial exposure of the bone is not complete. Therefore, we consider the condition of BP/1/3849 as representative of *Olivierosuchus*.

The proximodistally elongated distal carpal 1 could be interpreted as functionally equivalent to an McII–V due to its distal location relative to other distal carpals and due to its proportions within the first ray. This interpretation is congruent with the functional equivalence of the first metacarpal and the first phalanx of the lateral digits in non-mammaliaform synapsids, as proposed by Kümmell and Frey (2014) in their analysis of the first ray. Distal extension of distal carpal 1 to the metacarpus is also recognized in several mammals of different lineages, including *Ornithorhynchus*, *Hylobates*, *Lepus*, *Castor*, and *Priodontes* (Lessertisseur and Saban, 1967).

Elongation of distal carpal 1, which displaces McI distally, not only contributes to the length of the first ray but also is responsible for the asymmetry of the carpometacarpal line (Fig. 3). Thus, a deviation of the arch formed by the series of carpometacarpal joints is generated in the first ray. This pattern is particularly pronounced in *Tetracynodon* and *Olivierosuchus*. Kümmell and Frey (2014) have previously noted this pattern in Synapsida. They report that the distal carpal 1 is mostly aligned with the row of distal carpals 2–5 proximally and with the row of metacarpals II–V distally. Even in cases of small and quadrangular expressions of distal carpal 1 within Therocephalia, the carpometacarpal line is displaced distally in the first ray (see Fig. 3D).

Metacarpal Patterns

The therocephalians analyzed here exhibit the common amniote pattern of metacarpal length disparity, in which metacarpals increase from McI to McIV, followed by a decrease to McV (Romer, 1956; Kardong, 2011; Fig. 7A–E). Although this pattern is undoubtedly present in Therocephalia, the length disparity between the metacarpals in the metacarpal series is intermediate in a disparity-uniformity gradient observed through Synapsida. This demonstrates a trend towards equalization of metacarpal lengths during synapsid phylogenetic history. Thus, early synapsids, such as sphenacodontids, display great disparity in metacarpal length, a feature steadily reduced throughout the therapsid phylogenetic tree, leading to the condition of generalized mammals, which have a near uniform metacarpal length (Hopson, 1995). Hopson (1995) used the McII/McIV index as a proxy for disparity/uniformity, and he established a relationship between phalangeal reduction and metacarpal uniformity. He found that metacarpal length differences decreased in clades with the maximum degree of phalangeal reduction (with a McII/McIV index close to 1). However, he mentioned that there was only a low level of interaction of these two trends in achieving a symmetrical manus. Therocephalia has reached the maximum degree of phalangeal reduction and already possesses the mammalian

phalangeal formula, but the McIV/McII index assumes values of over 0.5 (Fig. 7), contrary to Hopson's (1995) proposed correlation.

The metacarpophalangeal line of Therocephalia (Fig. 3) shows a gradual increase from the first to the fourth ray, and a decrease from the fourth to the fifth, following the elongation pattern of the metacarpals. As can be deduced from the facets of the joints, the metacarpophalangeal joints exhibit more flexion and extension than the carpometacarpal joints. Additionally, absence in the metacarpal region of a dermic and an epidermic sheath packing the rays (as characterizes the manus palm) allows the metacarpal phalangeal joint to display a greater degree of mobility. The curvature of the metacarpophalangeal line is also critical in allowing a high degree of autopodial rotation, which compensates for the rotation transferred from the antebrachium to the manus during the propulsion phase of sprawling locomotion (Kümmell, 2009).

Behavioral Significance

Only a few therapsid taxa show overwhelming morphological evidence indicating digging ability. These are two closely related dicynodonts: *Cistecephalus* and *Kawingasaurus*. The strongest evidence in these cases derives from extremely modified (well-ossified) skulls, short and robust humeri with very expanded proximal and distal portions, ulnae with a conspicuous olecranon process, and a broad manus with broad digits (Cox, 1972; Cluver, 1978). No other non-mammaliaform therapsids present such strong skeletal evidence for a burrowing lifestyle, although the robust humerus, anteroposteriorly widened scapula, and large, wide, spatulate terminal phalanges of the manus of *Lystrosaurus* have been interpreted as being consistent with burrowing (Botha-Brink, 2017). *Cistecephalus* is reconstructed as a shovel digger based on its broad, shovel-like manus, with basal phalanges that are wider than long and very long unguals. It probably performed humeral rotation digging like *Talpa* and *Tachyglossus*, which would be consistent with its long olecranon process and the wide distal end of its humerus (Kümmell, 2009). Shovel digging performed by humeral rotation is not indicated for *Tetracynodon* AM 3677, which is morphologically considerably different from *Cistecephalus*. *Tetracynodon* AM 3677, with its long humerus and antebrachium and long metacarpals III–V, is not equipped for shovel digging. However, it is well adapted to perform scratch-digging (see below).

The presence of elongated digits III and IV having equal length in AM 3677 resembles the condition seen in some extant digging amniotes. For example, the amphisbaenian *Bipes* and the edentate *Dasyurus* have a pair of elongated digits reaching equal length, although in these taxa the digits are II and III (*Dasyurus* additionally having lost the fifth finger; Kley and Kearney, 2007). In all three cases, the elongated digits are represented by three phalanges, being a clear case of phalangeal reduction in the amphisbaenian (Fedak and Hall, 2004; Shapiro et al., 2007). In these extant diggers, the great ungual phalanges contribute fundamentally to the elongation of the two longest digits in the manus. In *Tetracynodon*, the McIII is shorter than McIV and the ungual phalanx III is remarkably elongated. Therefore, the trade-off for the acquisition of two digits similar in length is achieved through variation in the relative proportions between the metacarpals and unguals, with the remaining elements remaining uniform. In *Dasyurus*, this condition is acquired through the variation of different phalangeal lengths in digits II and III (see Kley and Kearney, 2007). In *Bipes*, ray III is slightly shorter than ray II because the ungual of digit III is slightly shorter than that of digit II. Experimental work shows that two or more digits can work together as a functional unit. Such digits are usually called a virtual finger (Iberall, 1997; Feix et al., 2015). The third and fourth digits

in *Tetracynodon* may have acted as a virtual finger as suggested by their uniformity of length. This unit would have increased the efficiency of the forces applied for the movement of the system. The two digits working together as a unit in *Tetracynodon* would correspond to an increase in the stockiness of the manual elements. It has been suggested, that in scratch-diggers all claws flex as a unit, helped by the sesamoids and tendons of the manus (Hildebrand, 1985). The virtual finger increases the transmission of forces applied on the substrate. The structure of *Tetracynodon*'s digits thus strongly suggests that its manus was used for digging.

In addition to the evidence outlined above, *Tetracynodon* has laterally compressed unguals, another feature typical of scratch-diggers (Hildebrand, 1985). In terms of the behavioral classification of digging by Hildebrand (1985), *Tetracynodon* would have been a scratch-digger, extending the forefeet anteriorly and flexing the middle and ungual joints, so that the claws were directed downward to the substrate. In extant vertebrate diggers with abducted limbs, the manus is moved relatively slowly in lateral ellipses around the body during scratching (Hildebrand, 1985; Hildebrand and Goslow, 2001), a pattern that was also suggested for most non-mammaliaform therapsid diggers (Kümmell, 2009). Modification of the muscles in these animals would have been necessary to increase strength for flexing the larger digits and the wrist (Hildebrand, 1985).

The ungual phalanx-digital index for digit III is defined as the length of the phalanx III ungual as a percentage of the entire length of digit III (Kümmell, 2009). With a value of 54%, *Tetracynodon* AM 3677 shows the highest value for any therocephalian studied thus far. Living scratch-digger animals usually have high values for this index (e.g., 73% for *Dasyurus*, 58% for *Manis*, and 51% for the amphisbaenian *Bipes*). In nonfossorial terrestrial and arboreal forms, this index tends to be smaller (e.g., 30% in *Didelphis*, 28% in *Sciurus*, and 24% in the arboreal anomodont *Suminia*). The climbing method of those few climbers with long ungual phalanges (members of Pilosa) would not be an option for *Tetracynodon*. The long unguals of *Tetracynodon* in the third and fourth rays therefore provide strong support for digging ability in this taxon.

The length-to-width index of the basal phalanx of digit IV (= length/width index or LWI) is one of the best lifestyle predictors (Weisbecker and Warton, 2006; Kümmell, 2009; Kümmell and Frey, 2012). Low LWI values indicate reduced potential for bending of the relevant bone and good resistance to torsion. Accordingly, wide and short basal phalanges usually characterize diggers. However, the LWI is weight dependent. Bigger animals show comparatively higher values than do smaller forms with similar behavior, so that size has to be considered during reconstruction. Additionally, Therocephalia as a group have relatively low LWI values among Therapsida, probably due to their peculiar locomotor mode (Kümmell, 2009). So, it is noteworthy that the LWI value of *Tetracynodon* AM 3677 is considerably lower than those of other small Therocephalia, showing that *Tetracynodon* is better equipped for a digging lifestyle. We have shown, that among extant marsupials, the LWI value of *Tetracynodon* AM 3677 more closely resembles those of the diprotodontid diggers *Bettongia penicillata* and *Potorous* than those of the terrestrial diprotodontids *Lagorchestes hirsutus* and *Onychogalea lunata* (Fig. 5). Moreover, the body length estimated for *T. darti* AM 3677 (~38 cm; our data) is similar to that of *Bettongia penicillata* and *Potorous*. Notably, both the proportion of the basal phalanx of the fourth digit and the body size of *T. darti* AM 3677 are similar to the condition in the latter potoroid diprotodontids. *Bettongia* and *Potorous* maintain a bipedal posture during fast locomotion, so they do not need to use their manus when running quickly. Thus, their forelimbs are well equipped for scratch-digging and for the manipulation of items. Compared

with the scratch-diggers of other therapsid clades, it is clear that the LWI values of *Tetracynodon* are in the lower range. Kümmell (2009) recovered the dicynodont *Diictodon* (LWI = 2.11, 2.12, 2.46), the basal non-mammaliaform cynodont *Procynosuchus* RC 92 (LWI = 1.71), and *Thrinaxodon* (LWI = 2.81–4.38) as scratch-diggers. The LWI for *Tetracynodon* AM 3677 is 1.79, a value close to the values of the aforementioned forms or clearly below them. Similarly, Lyson et al. (2016) used the presence of a large manus with short nonterminal phalanges as a criterion for fossoriality. This combination of a large manus with short nonterminal phalanges is also represented in the manus of AM 3677, providing further evidence for a digging function in *Tetracynodon*.

Notably, several burrowing forms of different sizes have been described from the Lower Triassic of the Karoo Basin (Groenewald et al., 2001; Damiani et al., 2003a; Fernandez et al., 2013; Botha-Brink, 2017). All this combined evidence adds weight to the idea that burrowing in the aftermath of the end-Permian environmental crisis may have served as an important survival strategy for Early Triassic therapsids (Smith and Botha, 2005; Smith and Botha-Brink, 2014; Lyson et al., 2016; Huttenlocker and Farmer, 2017; Jasinowski and Abdala, 2017).

ACKNOWLEDGMENTS

We acknowledge the encouragement of V. Abdala for the development of this research. Skillful preparation of the focal specimen, as well as several other therapsid manuses, was performed by C. Dube and T. Nemavhundi at the Evolutionary Studies Institute, Johannesburg. We are grateful to the curators of the visited collections for access to the specimens. We thank editors J. Harris and J. Botha-Brink, and the reviewers A. Huttenlocker and C. Kammerer, who contributed valuable ideas that improved this work. F.A.'s research is funded by the National Research Foundation (NRF), South Africa; F.A. and G.F. are funded by the Consejo Nacional de Investigaciones Científicas y Técnicas (CONICET), Argentina. Research by R.G. is supported by the South African NRF-DST Centre for Excellence in Palaeosciences (CoEPal) and the Millennium Trust. Research trips of G.F. and S.K. to South Africa were financed by incentive research funds from the NRF to F.A.

LITERATURE CITED

- Abdala, F., B. Rubidge, and J. van den Heever. 2008. The oldest therocephalians (Therapsida, Eutheriodonta) and the early diversification of Therapsida. *Palaeontology* 51:1011–1024.
- Abdala, F., T. Jashashvili, B. S. Rubidge, and J. van den Heever. 2014a. New material of *Microgomphodon oligocynus* (Eutherapsida, Therocephalia) and the taxonomy of southern African Bauriidae; pp. 209–231 in C. Kammerer, K. Angielczyk, and J. Fröbisch (eds.), *Early Evolutionary History of the Synapsida*. Springer, Dordrecht, The Netherlands.
- Abdala, F., C. F. Kammerer, M. O. Day, S. Jirah, and B. S. Rubidge. 2014b. Adult morphology of the therocephalian *Simorhinella baini* from the Karoo Basin, South Africa and the taxonomy, geographic and temporal distribution of the Lycosuchidae. *Journal of Paleontology* 88:1139–1153.
- Attridge, J. 1956. The morphology and relationships of a complete therocephalian skeleton from the *Cistecephalus* Zone of South Africa. *Proceedings of the Royal Society of Edinburgh B* 4:59–93.
- Berner, R. A., J. M. VandenBrooks, and P. D. Ward. 2007. Oxygen and evolution. *Science* 316:557–558.
- Boonstra, L. D. 1934. A contribution to the morphology of the mammal-like reptiles of the suborder Therocephalia. *Annals of the South African Museum* 31:215–267.
- Boonstra, L. D. 1964. The girdles and limbs of the pristerognathid Therocephalia. *Annals of the South African Museum* 48:121–165.
- Bordy, E. M., O. Sztanó, B. S. Rubidge, and A. Bumby. 2011. Early Triassic vertebrate burrows from the Katberg Formation of the south-western Karoo Basin, South Africa. *Lethaia* 44:33–45.
- Botha-Brink, J. 2017. Burrowing in *Lystrosaurus*: preadaptation to a postextinction environment? *Journal of Vertebrate Paleontology*. doi: 10.1080/02724634.2017.1365080.
- Botha-Brink, J., and S. P. Modesto. 2011. A new skeleton of the therocephalian synapsid *Olivierosuchus parringtoni* from the Lower Triassic South African Karoo Basin. *Palaeontology* 54:591–606.
- Botha-Brink, J., F. Abdala, and A. Chinsamy. 2012. The radiation and osteohistology of nonmammaliaform cynodonts; pp. 223–246 in A. Chinsamy-Turan (ed.), *Forerunners of Mammals: Radiation, Histology, Biology*. Indiana University Press, Bloomington, Indiana.
- Carroll, R. L., and R. Holmes. 2007. Evolution of the appendicular skeleton of amphibians; pp. 225–244 in B. K. Hall (ed.), *Fins into Limbs: Evolution, Development and Transformation*. University of Chicago Press, Chicago, Illinois.
- Cihák, R. 1972. Ontogenesis of the skeleton and intrinsic muscles of the human hand and foot. *Ergebnisse der Anatomie und Entwicklungsgeschichte* 46:5–194.
- Cluver, M. A. 1969. *Zorillodontops*, a new scaloposaurid from the Karoo. *Annals of the South African Museum* 52:183–188.
- Cluver, M. A. 1978. The skeleton of the mammal-like reptile *Cistecephalus* with evidence for a fossorial mode of life. *Annals of the South African Museum* 76:213–246.
- Cox, C. B. 1972. A new digging dicynodont from the Upper Permian of Tanzania; pp. 173–189 in K. A. Joysey and T. S. Kemp (eds.), *Studies in Vertebrate Evolution*. Oliver and Boyd, Edinburgh, U.K.
- Damiani, R., S. Modesto, A. Yates, and J. Neveling. 2003a. Earliest evidence of cynodont burrowing. *Proceedings of the Royal Society of London B. Biological Sciences* 270:1747–1751.
- Damiani, R., J. Neveling, S. Modesto, and A. Yates. 2003b. Barendskraal, a diverse amniote locality from the *Lystrosaurus* Assemblage Zone, Early Triassic of South Africa. *Palaeontologia africana* 39:53–62.
- Fabrezi, M., V. Abdala, and M. I. Martínez Oliver. 2007. Developmental basis of limb homology in lizards. *Anatomical Record* 290:900–912.
- Fernandez, V., F. Abdala, K. J. Carlson, D. C. Cook, B. S. Rubidge, A. Yates, and P. Tafforeau. 2013. Synchrotron reveals Early Triassic odd couple: injured amphibian and aestivating therapsid share burrow. *PLoS ONE* 8:e64978.
- Fedak, T. J., and B. Hall. 2004. Perspectives on hyperphalangy: patterns and processes. *Journal of Anatomy* 204:151–163.
- Flower, W. H. 1885. *An Introduction to the Osteology of the Mammalia*. Macmillan and Co., London, 412 pp.
- Fourie, H., and B. S. Rubidge. 2007. The postcranial skeletal anatomy of the therocephalian *Regisaurus* (Therapsida: Regisauridae) and its utilization for biostratigraphic correlation. *Palaeontologia africana* 42:1–16.
- Fourie, H., and B. S. Rubidge. 2009. The postcranial skeleton of the basal therocephalian *Glanosuchus macrops* (Scylacosauridae) and comparison of morphological and phylogenetic trends amongst Theriodontia. *Palaeontologia africana* 44:27–39.
- Fröbisch, J., and R. R. Reisz. 2009. The late Permian herbivore *Suminia* and the early evolution of arboreality in terrestrial vertebrate ecosystems. *Proceedings of the Royal Society B. Biological Sciences* 276:3611–3618.
- Fröbisch, J., and R. R. Reisz. 2011. The postcranial anatomy of *Suminia getmanovi* (Synapsida: Anomodontia), the earliest known arboreal tetrapod. *Zoological Journal of the Linnean Society* 62:661–698.
- Gates, S. M., and K. M. Middleton. 2007. Skeletal adaptations for flight; pp. 225–244 in B. K. Hall (ed.), *Fins into Limbs: Evolution, Development and Transformation*. University of Chicago Press, Chicago, Illinois.
- Groenewald, G. H., J. Welman, and J. A. MacEachern. 2001. Vertebrate burrow complexes from the Early Triassic *Cynognathus* Zone (Driekoppen Formation, Beaufort Group) of the Karoo Basin, South Africa. *Palaios* 16:148–160.
- Feix, T., J. Romero, H. B. Schmiedmayer, A. M. Dollar, and D. Kragic. 2015. The grasp taxonomy of human grasp types. *IEEE Transactions on Human-Machine Systems* 46:66–77.

- Hildebrand, M. 1985. Digging in quadrupeds; pp. 89–109 in M. Hildebrand, D. M. Bramble, K. F. Liem, and D. B. Wake (eds.), *Functional Vertebrate Morphology*. Belknap Press, Cambridge, Massachusetts.
- Hildebrand, M., and G. E. Goslow. 2001. *Analysis of Vertebrate Structure*, fifth edition. Wiley, New York, 635 pp.
- Holmgren, N. 1952. An embryological analysis of the mammalian carpus and its bearing upon the question of the origin of the tetrapod limb. *Acta Zoologica* 33:1–115.
- Hopson, J. A. 1995. Patterns of evolution in the manus and pes of non-mammalian therapsids. *Journal of Vertebrate Paleontology* 15:615–639.
- Huttenlocker, A. K. 2014. Body size reductions in nonmammalian eutheriodont therapsids (Synapsida) during the End-Permian mass extinction. *PLoS ONE* 9:e87553.
- Huttenlocker, A. K., and J. Botha-Brink. 2013. Body size and growth patterns in the therocephalian *Moschorhinus kuchingi* (Therapsida: Eutheriodontia) before and after the End-Permian extinction in South Africa. *Paleobiology* 39:253–277.
- Huttenlocker, A. K., and J. Botha-Brink. 2014. Bone microstructure and the evolution of growth patterns in Permo-Triassic therocephalians (Amniota, Therapsida) of South Africa. *PeerJ* 2:e325.
- Huttenlocker, A. K., and C. G. Farmer. 2017. Bone microvasculature tracks red blood cell size diminution in Triassic mammal and dinosaur forerunners. *Current Biology* 27:48–54.
- Huttenlocker, A. K., and C. A. Sidor. 2016. The first karenitid (Therapsida, Therocephalia) from the Upper Permian of Gondwana and the biogeography of Permo-Triassic therocephalians. *Journal of Vertebrate Paleontology*. doi: 10.1080/02724634.2016.1111897.
- Huttenlocker, A. K., C. A. Sidor and R. M. H. Smith. 2011. A new specimen of *Promoschorhynchus* (Therapsida: Therocephalia: Akidnognathidae) from the Lower Triassic of South Africa and its implications for theriodont survivorship across the Permo-Triassic boundary. *Journal of Vertebrate Paleontology* 31:405–421.
- Iberall, T. 1997. Human prehension and dexterous robot hands. *International Journal of Robotics Research* 16:285–299.
- Jablonsky, D. 2005. Mass extinctions and macroevolution. *Paleobiology* 31:192–210.
- Jasinowski, S. C., and F. Abdala. 2017. Aggregations and parental care in the Early Triassic basal cynodonts *Galesaurus planiceps* and *Thrinaxodon liorhinus*. *PeerJ* 5:e2875.
- Kardong, K. 2011. *Vertebrates: Comparative Anatomy, Function, Evolution*, sixth edition. McGraw-Hill, San Francisco, California, 800 pp.
- Kemp, T. S. 1983. The relationships of mammals. *Zoological Journal of the Linnean Society* 77:353–384.
- Kinlaw, A. 1999. A review of burrowing by semi-fossorial vertebrates in arid environments. *Journal of Arid Environments* 41:127–145.
- Kley, N. J., and M. Kearney 2007. Adaptations for digging and burrowing; pp. 284–309 in B. K. Hall (ed.), *Fins into Limbs: Evolution, Development, and Transformation*. University of Chicago Press, Chicago, Illinois.
- Kümmell, S. B. 2009. Die Digiti der Synapsida: Anatomie, Evolution und Konstruktionsmorphologie. Ph.D. dissertation, Universität Witten/Herdecke, Witten, Germany, 424 pp.
- Kümmell, S. B., and E. Frey. 2012. What digits tell us about digging, running and climbing in recent and fossil Synapsida; pp. 117–118 in 10th Annual Meeting of the European Association of Vertebrate Palaeontologists. (19–24 June 2012). Teruel, Spain
- Kümmell, S. B., and E. Frey. 2014. Range of movement in ray I of manus and pes and the prehensibility of the autopodia in the Early Permian to Late Cretaceous non-anomodont Synapsida. *PLoS ONE* 9:e113911.
- Lessertisseur, J., and R. Saban. 1967. Squelette appendiculaire; pp. 709–1078 in P. P. Grassé (ed.), *Traité de Zoologie*. Tome 16, fascicule I. Masson et Cie, Paris.
- Lyson, T. R., B. S. Rubidge, T. M. Scheyer, K. de Queiroz, E. R. Schachner, R. M. H. Smith, J. Botha-Brink, and G. S. Bever. 2016. Fossorial origin of the turtle shell. *Current Biology* 26:1887–1894.
- Liu, J., and F. Abdala. 2015. New discoveries from the *Sinokannemeyeria-Shansisuchus* Assemblage Zone: 2. A new species of *Nothogomphodon* (Therapsida: Therocephalia) from the Ermaying Formation of Shanxi, China. *Vertebrata Palasiatica* 53:123–132.
- Modesto, S. P., and J. Botha-Brink. 2010. A burrow cast with *Lystrosaurus* skeletal remains from the Lower Triassic of South Africa. *Journal of Vertebrate Paleontology* 25:274–281.
- Polly, P. D. 2007. Limbs in mammalian evolution; pp. 225–244 in B. K. Hall (ed.), *Fins into Limbs: Evolution, Development, and Transformation*. University of Chicago Press, Chicago, Illinois.
- Prochel, J., S. Begal, and H. Burda. 2014. Morphology of the carpal region in some rodents with special emphasis on hystricognaths. *Acta Zoologica* 95:220–238.
- R Development Core Team. 2011. R: a language and environment for statistical computing. The R Foundation for Statistical Computing, Vienna, Austria. Available at www.R-project.org. Accessed February 14, 2016.
- Rieppel, O. 1992. Studies on skeleton formation in reptiles. III. Patterns of ossification in the skeleton of *Lacerta vivipara* Jacquin (Reptilia, Squamata). *Fieldiana: Zoology*, new series 68:1–25.
- Romer, A. S. 1956. *Osteology of the Reptiles*. University of Chicago Press, Chicago, Illinois, 722 pp.
- Roopnarine, P. D., and K. D. Angielczyk. 2015. Community stability and selective extinction during the Permian-Triassic mass extinction. *Science* 350:90–93.
- Rubidge, B. S. 2013. The roots of early mammals lie in the Karoo: Robert Broom’s foundation and subsequent research progress. *Transactions of the Royal Society of South Africa* 68:41–52.
- Shapiro, M. D., N. H. Shubin, and J. P. Downs. 2007. Limb diversity and digit reduction in reptilian evolution; pp. 225–244 in B. K. Hall (ed.), *Fins into Limbs: Evolution, Development, and Transformation*. University of Chicago Press, Chicago, Illinois.
- Sigogneau, D. 1963. Note sur une nouvelle espèce de Scaloposauridae. *Palaeontologia africana* 8:13–37.
- Sigurdsen, T., A. K. Huttenlocker, S. P. Modesto, T. Rowe, and R. J. Damiani. 2012. Reassessment of the morphology and paleobiology of the therocephalian *Tetracynodon darti* (Therapsida), and the phylogenetic relationships of Baurioidea. *Journal of Vertebrate Paleontology* 32:1113–1134.
- Shubin, N. H., and P. Alberch. 1986. A morphogenetic approach to the origin and basic organization of the tetrapod limb. *Evolutionary Biology* 20:319–387.
- Smith, R. M. H., and J. Botha. 2005. The recovery of terrestrial vertebrate diversity in the South African Karoo Basin after the end-Permian extinction. *Comptes Rendus Palevol* 4:623–636.
- Smith R. M. H., and J. Botha-Brink. 2014. Anatomy of a mass extinction: sedimentological and taphonomic evidence for drought-induced die-offs at the Permo-Triassic boundary in the main Karoo Basin, South Africa. *Palaeogeography, Palaeoclimatology, Palaeoecology* 396:99–118.
- Sun, Y., M. M. Joachimski, P. B. Wignall, C. Yan, Y. Chen, H. Jiang, L. Wang, and X. Lai. 2012. Lethally hot temperatures during the Early Triassic greenhouse. *Science* 338:366–370.
- Watson, D. M. S. 1931. On the skeleton of a bauriamorph reptile. *Proceedings of the Zoological Society of London* 101:1163–1205.
- Weisbecker, V., and M. Sánchez-Villagra. 2006. Carpal evolution in diprotodontian marsupials. *Zoological Journal of the Linnean Society* 146:369–384.
- Weisbecker, V., and D. I. Warton. 2006. Evidence at hand: diversity, functional implications, and locomotor prediction in intrinsic hand proportions of diprotodontian marsupials. *Journal of Morphology* 267:1469–1485.

Submitted July 27, 2017; revisions received April 27, 2018; accepted May 12, 2018.

Handling editor: Jennifer Botha-Brink.